ORGANOMETALLICS

Article

pubs.acs.org/Organometallics

Mechanism of MTO-Catalyzed Deoxydehydration of Diols to Alkenes Using Sacrificial Alcohols

Shuo Liu,[†] Aysegul Senocak,[†,§] Jessica L. Smeltz,[‡] Linan Yang,[†] Benjamin Wegenhart,[†] Jing Yi,[†] Hilkka I. Kenttämaa,[†] Elon A. Ison,[‡] and Mahdi M. Abu-Omar*[,†]

[†]Brown Laboratory and Department of Chemistry, Purdue University, 560 Oval Drive, West Lafayette, Indiana 47907, United States

[‡]Department of Chemistry, North Carolina State University, Raleigh, North Carolina 27695, United States

Supporting Information

ABSTRACT: Catalytic deoxydehydration (DODH) of vicinal diols is carried out employing methyltrioxorhenium (MTO) as the catalyst and a sacrificial alcohol as the reducing agent. The reaction kinetics feature an induction period when MTO is added last and show zero-order in [diol] and half-order dependence on [catalyst]. The rate-determining step involves reaction with alcohol, as evidenced by a KIE of 1.4 and a large negative entropy of activation ($\Delta S^{\ddagger} = -154 \pm 33$ J mol^{-1} K^{-1}). The active form of the catalyst is methyldioxorhenium(V) (MDO), which is formed by reduction of MTO by alcohol or via a novel C−C bond cleavage of an MTO-diolate complex. The majority of the MDO-diolate complex is present in dinuclear form, giving rise to the $[Re]^{1/2}$ dependence. The MDO-diolate complex undergoes further reduction by alcohol in the rate-determining step to give rise to a putative rhenium(III) diolate. The latter is the active species in DODH extruding stereoselectively *trans*-stilbene from (*R*,*R*)-(+)-hydrobenzoin to regenerate MDO and complete the catalytic cycle.

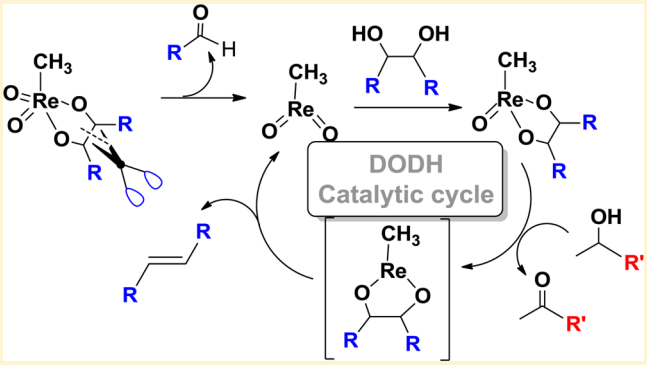

The development of renewable energy sources has become an important research field because of dwindling fossil fuel supplies and concerns over greenhouse gas emissions. Biomass represents an attractive and sustainable platform for the production of liquid fuels and valuable chemicals through deoxygenation of biomass-derived polyols and sugar alcohols.[1] A promising route toward this goal is catalytic deoxydehydration (DODH) of vicinal diols to alkenes employing rhenium-based catalysts. Nonetheless, there are only a few studies dealing with DODH in comparison with the reverse reaction, dihydroxylation of alkenes, which is a widely used reaction in organic synthesis and industry.[2] Two organometallic oxorhenium complexes have been reported to catalyze the deoxygenation of epoxides and deoxydehydration of diols to alkenes.[3] Cook and Andrews reported catalytic deoxydehydration of diols with [Cp*Re^{V}(O)(diolate)] employing phosphines as reductants/oxygen atom acceptors.[4] Our group studied the conversion of diols and epoxides to alkenes using molecular hydrogen (H_2) and methyltrioxorhenium(VII) (MTO) as the catalyst.[5] Subsequently, Bergman and coworkers employed sacrificial alcohols as the hydrogen source with $Re_2(CO)_{10}$ as a catalyst,[6] and the Nicholas group used sulfite as a reducing equivalent in the presence of several oxorhenium catalysts.[7] Fernandes et al. reported on rhenium-catalyzed deoxygenation of epoxides without the use of a reducing agent.[8] Most recently and independently, our group as well as Toste's reported rhenium-catalyzed DODH and transfer hydrogenation of biomass-derived glycerol, polyols, and sugar alcohols.[9,10]

In addition, Schlaf and Bullock have pioneered the use of organometallic ruthenium catalysts for the deoxygenation of alcohols.[11] Srivastava's group has also utilized $(Cp^*Ru(CO)_2)_2$ for hydrodeoxygenation (HDO) and hydrocracking of diols and epoxides.[12]

Despite the recent flurry of studies dealing with catalytic deoxydehydration of diols, there have been limited kinetic investigations aimed at understanding the reaction mechanism under relevant catalytic conditions. Previous studies by our group and others had indicated two possible reaction pathways. These are illustrated in Scheme 1.[5,7,9,13] Pathway A invokes formation of rhenium(VII) diolate, which undergoes reduction to form Re^{V} diolate, followed by alkene extrusion to complete the catalytic cycle. Alternatively, pathway B proceeds by MTO reduction first with the sacrificial alcohol to afford methyldioxorhenium(V) (MDO), which coordinates the diol to give Re^{V} diolate. Both cycles share a common alkene-forming step from Re^{V} diolate (MDO·diolate).

From systematic experimentation, we have come to the realization that employing sacrificial alcohols as reductants represents a good system for detailed mechanistic and kinetic study of the MTO-catalyzed DODH reaction (eq 1). The

Received: February 13, 2013

   dx.doi.org/10.1021/om400127z | *Organometallics* XXXX, XXX, XXX−XXX

Scheme 1. Proposed Literature Mechanisms for DODH of Vicinal Diols to Alkenes Catalyzed by MTO

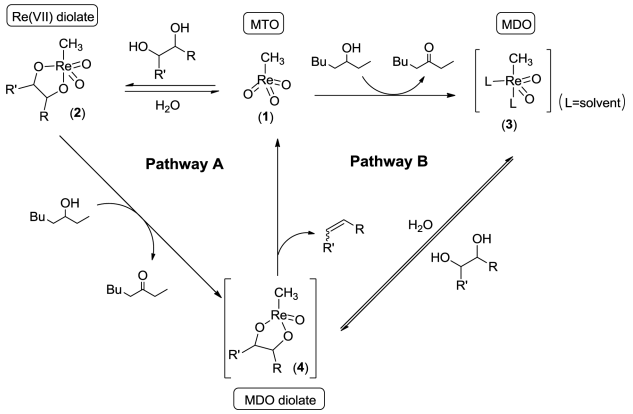

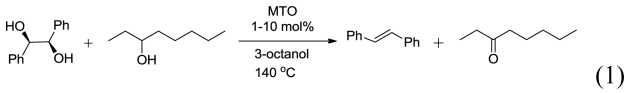

(1)

reaction proceeds smoothly under ambient pressure, open to air, in comparison to other systems that require high-pressure reactors. Here we present a thorough study of the rhenium-catalyzed DODH mechanism focusing on (*R*,*R*)-(+)-hydrobenzoin as the representative glycol substrate. We have chosen this substrate to study due to the stability of its product, *trans*-stilbene, under the reaction conditions. The reaction is zero-order in terms of (*R*,*R*)-(+)-hydrobenzoin and has an induction period when MTO is employed as the starting catalyst. This induction period is significantly reduced when MDO is used as the starting catalyst. These results indicate that MDO is indeed part of the catalytic cycle, while MTO is not. Furthermore, the kinetic dependence on the catalyst concentration $[Re]_T$ is half-order. Even though both rhenium(VII) and rhenium(V) diolate complexes (**4** and **2** in Scheme 1) are observed, we present compelling evidence based on careful kinetic analysis that the active form of the catalyst that affords alkene is most likely rhenium(III) diolate. The catalytic reaction gives a primary kinetic isotope effect on the secondary alcohol 3-octanol (k_H/k_D = 1.4), which is consistent with the reduction step of rhenium(V) diolate **4** as part of the rate-determining step(s). Our mechanistic insight should aid henceforth in the design of appropriate rhenium and other metal catalysts for DODH of diols and polyols.

RESULTS AND DISCUSSION

Reactions of Glycols with Sacrificial Alcohols. We examined the reactivity of several glycols and epoxides with MTO utilizing 3-octanol as both the solvent and reductant. The results are listed in Table 1. A mixture of a given glycol (1 equiv) with excess 3-octanol (10 equiv) in the presence of MTO (2 mol %) as the catalyst at 140 or 170 °C gave 100% conversion and good to moderate yields of the corresponding alkene along with 3-octanone, with reaction times ranging from 24 to 60 min. Aromatic diols were found to be more reactive than aliphatic diols. In addition, *trans*-1,2-cyclooctanediol did not react, while *cis*-1,2-cyclooctanediol converted smoothly to the alkene; this stereoselectivity has been noted previously for the H_2-driven deoxygenation and other DODH.[5−7] Other secondary alcohols such as nonanol and cyclooctanol can also be used for DODH of vicinal diols and afford good alkene yields (Table 1, entries 10−12). The slower reaction time with 5-nonanol can be attributed to steric hindrance. Interestingly, primary and benzylic alcohols such as 1-heptanol, benzyl alcohol, 1-phenylethanol, and diphenylmethanol are not effective as sacrificial alcohols in this reaction system. 1-Heptanol did not afford 1-heptanal, but it can be used as a solvent for the conversion of (*R*,*R*)-(+)-hydrobenzoin to *trans*-stilbene per eq 2. In the absence of a suitable sacrificial alcohol,

Table 1. MTO-Catalyzed DODH of Vicinal Diols and Deoxygenation of Epoxides Using Sacrificial Secondary Alcohols[a]

Entry	Glycol or epoxide	Sacrificial alcohol	T (°C)	t[b] (min)	Major product	% Yield[c]
1	(R,R)-(+)-hydrobenzoin	3-octanol	140	33	trans-stilbene	80%
2	(S,S)-(-)-hydrobenzoin	3-octanol	140	33	trans-stilbene	80%
3	meso-hydrobenzoin	3-octanol	140	30	cis-stilbene	40%
4	1,2-decanediol	3-octanol	170	54	1-decene	67%
5	cis-1,2-cyclooctanediol	3-octanol	170	72	cyclooctene	64%
6	cis-stilbene oxide	3-octanol	140	30	trans-stilbene	83%
7	styrene oxide	3-octanol	140	30	styrene	56%
8	1-phenyl-1,2-ethanediol	3-octanol	140	30	styrene	60%
9[d]	meso-erythritol	3-octanol	170	60	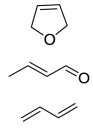	40%
10	(R,R)-(+)-hydrobenzoin	2-nonanol	140	40	trans-stilbene	80%
11	(R,R)-(+)-hydrobenzoin	cyclooctanol	170	21	trans-stilbene	70%
12	(R,R)-(+)-hydrobenzoin	5-nonanol	170	20	trans-stilbene	68%

[a]Reactions were carried out at 2.5 mmol of glycol with 10 equiv of sacrificial alcohol and 2 mol % MTO. [b]Refers to the time when the yield of the major product reached maximum. All conversions are 100%. [c]Yields of the major product(s) were determined by NMR using diphenylmethane as an internal standard. [d]Please refer to Supporting Information and ref 9 for details.

dx.doi.org/10.1021/om400127z | *Organometallics* XXXX, XXX, XXX−XXX

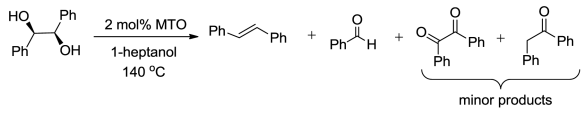

(2)

the DODH reaction proceeds using the substrate hydrobenzoin as a reductant. The product distribution includes *trans*-stilbene and benzaldehyde as major products and benzil and 1,2-diphenylethanone as minor products (eq 2; see Supporting Information).[6,12] Benzyl alcohol undergoes etherification to give dibenzyl ether, and 1-phenylethanol is dehydrated by MTO to give styrene.[13a,14]

Kinetic Measurements. Kinetic measurements on the progress of reaction were collected by heating a mixture of hydrobenzoin with excess 3-octanol (10 equiv) to 140 °C. The reaction was initiated by addition of 2, 5, or 10 mol % of MTO (method A; see Experimental Methods section for details). Aliquots were drawn at different times, quenched over ice, and analyzed by NMR and/or GC for determination of hydrobenzoin conversion and product yields. Figure 1a shows a representative kinetic profile for the disappearance of hydrobenzoin. The kinetics are characterized by an initial induction period (ca. 200 s) and zeroth-order dependence on [hydrobenzoin], as evidenced by the constant rate to more than 90% conversion. The zero-order dependence on substrate (*R*,*R*-hydrobenzoin) is indicative of a rate-determining step that involves active-catalyst formation or alkene extrusion.

Another method for examining the kinetics of the reaction is to add the substrate, hydrobenzoin, last to a heated solution of MTO (catalyst) and 3-octanol (method B). Here, a mixture of 3-octanol (10 equiv relative to diol) with a catalytic amount MTO was heated to 140 °C for 10 min, at which point the

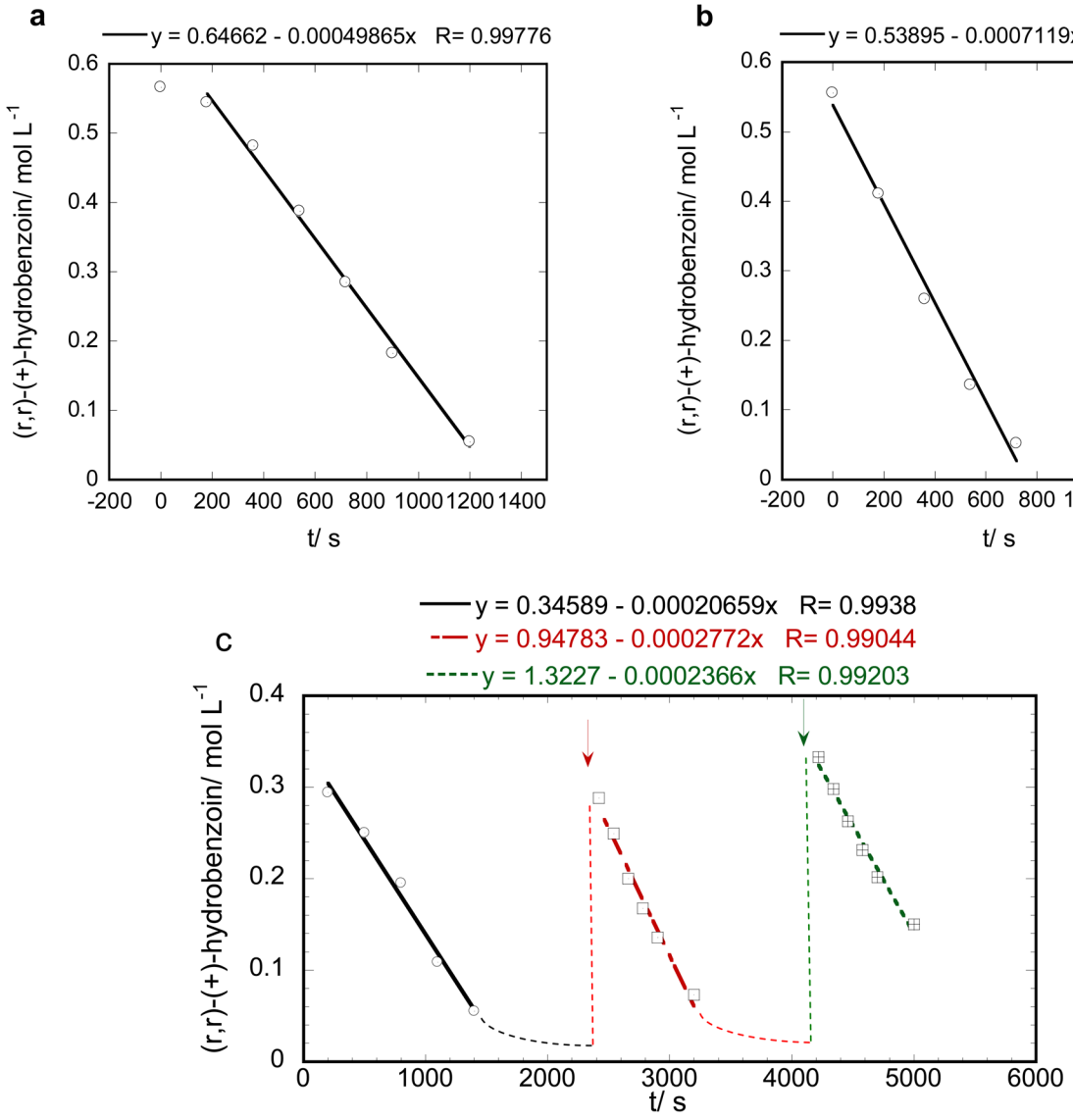

Figure 1. (a) Kinetic profile for DODH reaction of hydrobenzoin in 3-octanol at 140 °C. Conditions: 2.5 mmol of hydrobenzoin with ~25 mmol of 3-octanol preheated to 140 °C, MTO (0.05 mmol) added last (method A); (b) kinetic profile for DODH of hydrobenzoin. Same conditions as in (a) except hydrobenzoin was added last after incubation of MTO in 3-octanol at 140 °C for 10 min; (c) kinetic profile for three consecutive catalytic reactions. First in circles represents 2.5 mmol of hydrobenzoin with 50 mmol of 3-octanol preheated to 140 °C with MTO (0.05 mmol) added last (induction period omitted). Second and third in squares and hatched-squares, respectively, were initiated by addition of 2.5 mmol of hydrobenzoin ca. 10−15 min after complete conversion of the substrate from the previous addition. Subsequent additions of substrate are designated by the arrows.

dx.doi.org/10.1021/om400127z | *Organometallics* XXXX, XXX, XXX−XXX

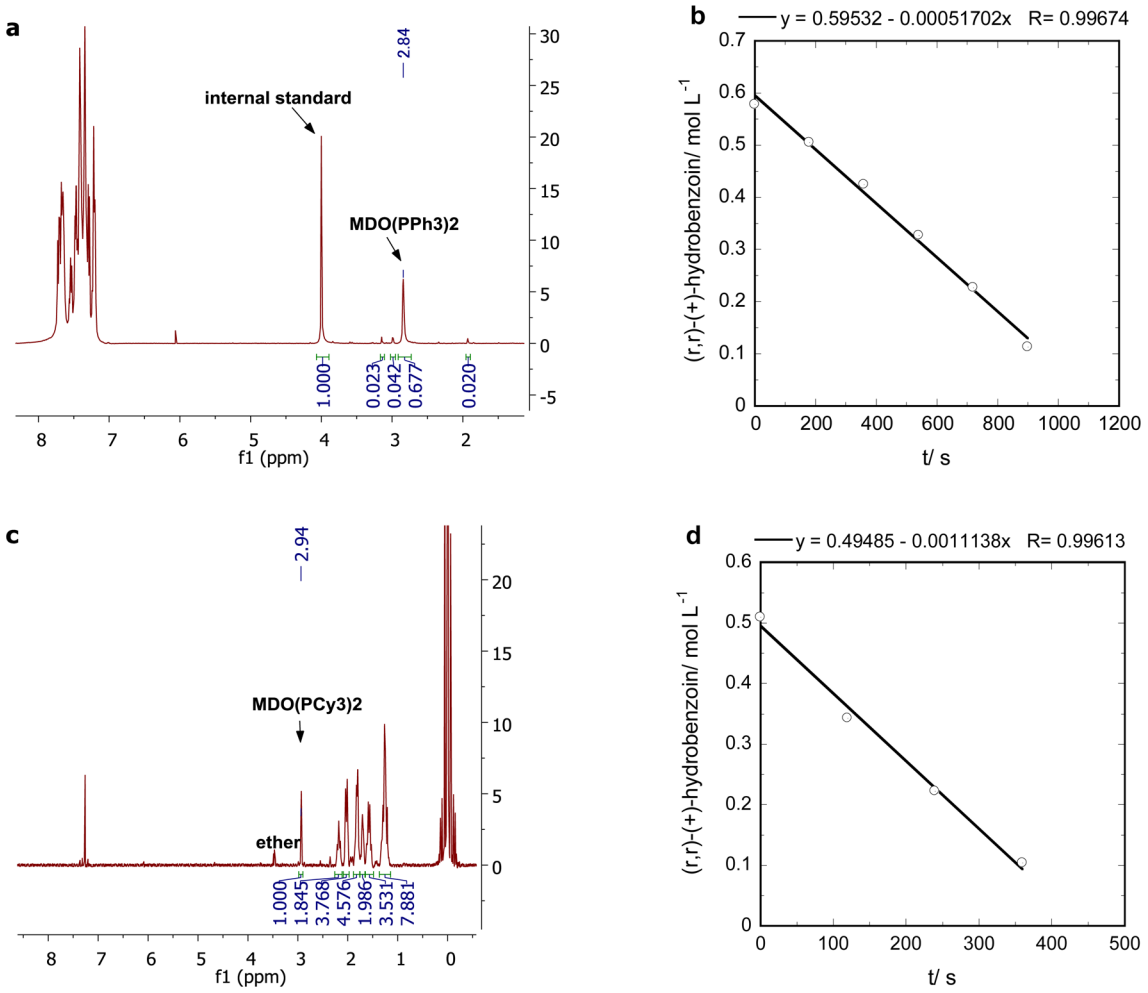

Figure 2. (a) ^{1}H NMR spectrum of MDO·$(PPh_3)_2$ in $CDCl_3$. The peak at ∼2.8 ppm refers to the methyl group on Re (Re−CH_3); the *y* axis is in arbitrary units. (b) Kinetic profile when using 2 mol % MDO·$(PPh_3)_2$ as the catalyst (preheated hydrobenzoin with 10 equiv of 3-octanol at 140 °C, catalyst added last, method A). (c) ^{1}H NMR spectrum of MDO·$(PCy_3)_2$ in $CDCl_3$. The peak at ∼2.9 ppm refers to the methyl group on Re (Re−CH_3). (d) Kinetic profile when using 10 mol % MDO·$(PCy_3)_2$ as the catalyst, using method A.

solution turned dark in color. The appropriate amount of hydrobenzoin was then added, and the reaction progress followed by collecting aliquots and analyzing them by NMR and GC. Figure 1b displays a typical kinetic profile for method B. The induction period was almost absent, and the observed rate (slope of the graph) was approximately 1.5× that in Figure 1a, where the catalyst was added last. It should be noted that the order of addition had no effect on the zeroth-order dependence on [hydrobenzoin]. Both profiles in Figure 1a and b show a constant rate throughout the reaction. The lack of induction period in Figure 1b is consistent with formation of the active catalyst from a reaction between MTO and 3-octanol. However, neither mechanism in Scheme 1 explains the observation of an induction period.

To probe the effect of reaction time on catalyst activity, we collected kinetic data for multiple reaction cycles starting with 20 equivalents of 3-octanol to hydrobenzoin. Since there would be more samples taken from the reaction mixtures, the amount of 3-octanol was increased to 20 equivalents. Ten to fifteen minutes after completion of the first reaction, another equivalent of hydrobenzoin was added to run a second catalytic cycle. After completion of the second cycle, a third catalytic cycle was commenced in the same manner. The results are shown in Figure 1c. An induction period was observed for the first cycle (omitted here), but no induction period was seen for the second and third cycles. Additionally, all three consecutive runs displayed zero-order dependence on [hydrobenzoin]. The rates of the second and third catalytic cycles were ca. 1.5× that of the first cycle, which is the rate with the active catalyst. In the same way, the rate collected by method B with hydrobenzoin added last (10 equiv of 3-octanol) is also 1.5 times faster than the rate collected by method A (10 equiv also) with MTO added last. All of these results are consistent with our notion that the active catalyst is generated by the reaction of MTO with 3-octanol, and there is little loss of activity even after 150 turnovers. Since the reactant concentrations of methods A and B are not the same, the rates (slopes) cannot be compared directly.

Extended reaction times of MTO with 3-octanol at 140 °C result in slow formation of a black precipitate, which has been identified as Re nanoparticles (see the Supporting Information for details).[15] The formed Re NPs can be isolated by filtration, and their activity was compared with that of the supernatant. The Re NPs were found to be much less active than the supernatant (filtrate). These findings are consistent with the active catalyst being homogeneous and not heterogeneous. Further validation of this premise was obtained from the Hg(0) poison test. Liquid mercury poisons the surface of heteroge-

dx.doi.org/10.1021/om400127z | *Organometallics* XXXX, XXX, XXX−XXX

neous metal catalysts.[16] If the reaction is not affected by the addition of mercury, such a result suggests a homogeneous reaction and *vice versa*. The kinetics of the reaction was compared in the presence of 10 equivalents of mercury present at the beginning of the reaction prior to catalyst addition. The rate of reaction and product selectivity were unaltered by the presence of mercury, which indicates that the active catalyst is homogeneous.

Experiments with Methyldioxorhenium(V) MDO. So far all indications point to reduction of MTO by the sacrificial alcohol. Therefore, MDO is a reasonable starting complex/catalyst to investigate. As MDO is not stable without ligation to ligands other than solvent molecules, we synthesized MDO·$(PPh_3)_2$ (Figure 2a) and MDO·$(PCy_3)_2$ (Figure 2c) from the reaction of MTO with PPh_3 and PCy_3, respectively, in organic solvent (see Experimental Methods section for details and single-crystal X-ray structures). MDO·$(PR_3)_2$ complexes were used as catalysts for the reaction of hydrobenzoin with 3-octanol at 140 °C. Kinetic measurements were collected according to method A; the catalyst was added last. As evident in Figure 2b and d, the reactions proceeded without an induction period and at a rate comparable to that observed for reactions starting with MTO. Furthermore, the dependence on [hydrobenzoin] was zeroth-order. These findings bode well with the hypothesis that MDO is involved in the catalytic cycle, but once it is formed, it does not return to MTO. In other words, MDO can be on the catalytic path but not via a cycle that involves MTO as suggested in Scheme 1.

Oxorhenium(VII) Diolate (2) and Its Potential Involvement. **2** was synthesized by the reaction of MTO and (*R*,*R*)-(+)-hydrobenzoin (1:1) in $CDCl_3$ in the presence of molecular sieves at room temperature.[17] The rhenium(VII) diolate was obtained in higher purity if the reaction was carried out in the dark by covering the flask with aluminum foil. The rhenium(VII) diolate (**2**) undergoes photodecomposition at room temperature (Scheme 2, reaction A). Complex **2** was

Scheme 2. Reactions of Rhenium Diolate at 140 °C

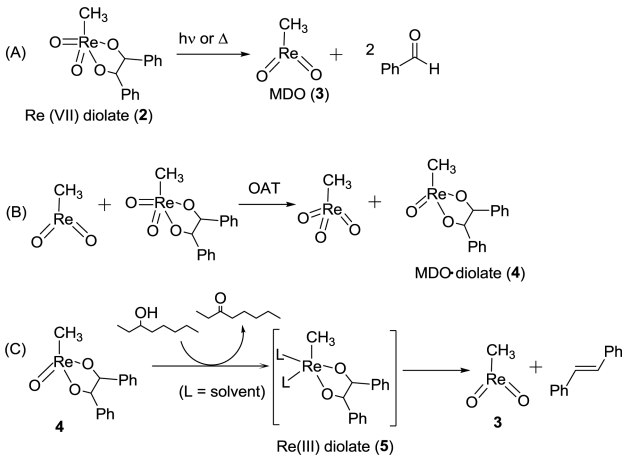

characterized by ^1H NMR. It shows resonances at 5.7 ppm for the diolato ring protons and a singlet at 2.7 ppm for the Re-CH_3 (Figure 3a). The structure of **2** was also characterized by mass spectrometric analysis of the reaction mixture in $CDCl_3$, a technique that has been used previously to study catalytic intermediates.[18] Upon ionization by atmospheric pressure chemical ionization (APCI), ions corresponding to attachment of a chloride anion to the diolate **2** were observed (see Experimental Methods section and Figure 8). The unique ion cluster pattern based on Cl and Re isotope distributions confirms the composition of the ion. A small amount of deprotonated Re(VII) diolate, probably formed via attachment of a chloride anion followed by the loss of HCl, was also observed. These results indicate the presence of diolate **2** in solution.

Heating a solution of **2** at 140 °C for 30 min produced MTO, MDO·diolate,[7a,10] and benzaldehyde but not stilbene (Figure 3b). Observation of ions corresponding to attachment of chloride anion to MTO, MDO, and MDO·diolate in the mass spectrometric analysis of the heated solution confirmed the presence of all three molecules (see Experimental Methods section and Figure 9). We offer reactions (A) and (B) in Scheme 2 as plausible pathways accounting for the observed products. Reaction (A) is triggered by heat, as well as by light at room temperature. Hence, the novel C−C cleaving reaction results from heat or light. MTO is formed from intermetallic oxygen atom transfer,[19] which was confirmed independently by adding MDO·$(PR_3)_2$ to **2** to give MTO and MDO·diolate (Figure 3d and Supporting Information). An important point herein that should not be overlooked is that despite the formation and observation of MDO·diolate, *trans*-stilbene was not produced. Therefore, it can be ascertained that MDO·diolate in the absence of a reductant does not extrude alkene by itself. Nevertheless, if the mixture of **2** and MDO·$(PR_3)_2$ is heated for a prolonged time (30 min), *trans*-stilbene is eventually produced but only after all of the rhenium(VII) diolate (**2**) has been consumed (Figure 4). Such an observation is consistent with autocatalysis. Furthermore, the rate constant for the formation of *trans*-stilbene from this mixture is quite slow (<0.000 58 s^{-1}) compared to the turnover frequency of a typical catalytic reaction, 0.0278 s^{-1}. In conclusion, Scheme 1, which involves the formation of **2** from MTO and the extrusion of stilbene from MDO·diolate, is refuted.

When 3-octanol was added to the mixture containing MTO and MDO·diolate, at 140 °C, *trans*-stilbene was produced along with 3-octanone (Figure 3c) within 30 min. On the basis of these observations, we propose that the MDO·diolate must be further reduced to form a rhenium(III) diolate, and the latter is responsible for alkene extrusion and regeneration of MDO (reaction (C) in Scheme 2).

The driving force is sufficient with alcohol under our conditions (140 °C) to form rhenium(III) diolate. Ison and co-workers have shown recently the formation of rhenium(III) acetate by reduction of oxorhenium(V) acyl with CO under mild conditions.[20] Interestingly, a recent computational study of the DODH reaction with MTO using H_2 as well as alcohols as reductants did not consider the involvement of rhenium(III).[21]

MDO is produced from the reaction of MTO and 3-octanol, accounting for the induction period observed when MTO is added last. Espenson et al. have shown that MDO could form a dimer $\mathbf{D}_1$.[22] Our own findings show further reduction to rhenium NPs at prolonged incubation at high temperature in 3-octanol. Carbon−carbon bond cleavage in rhenium(VII) diolate can also lead to MDO formation. MDO·diolate (**4**) reacts further with 3-octanol to provide a transient rhenium(III) that extrudes alkene and regenerates MDO. In addition, Re(V) diolate could also react with Re(III) diolate to form the dinuclear complex $\mathbf{D}_2$ or with itself to form a rhenium(V) diolate dimer $\mathbf{D}_3$. The evidence for these dinuclear rhenium

dx.doi.org/10.1021/om400127z | *Organometallics* XXXX, XXX, XXX−XXX

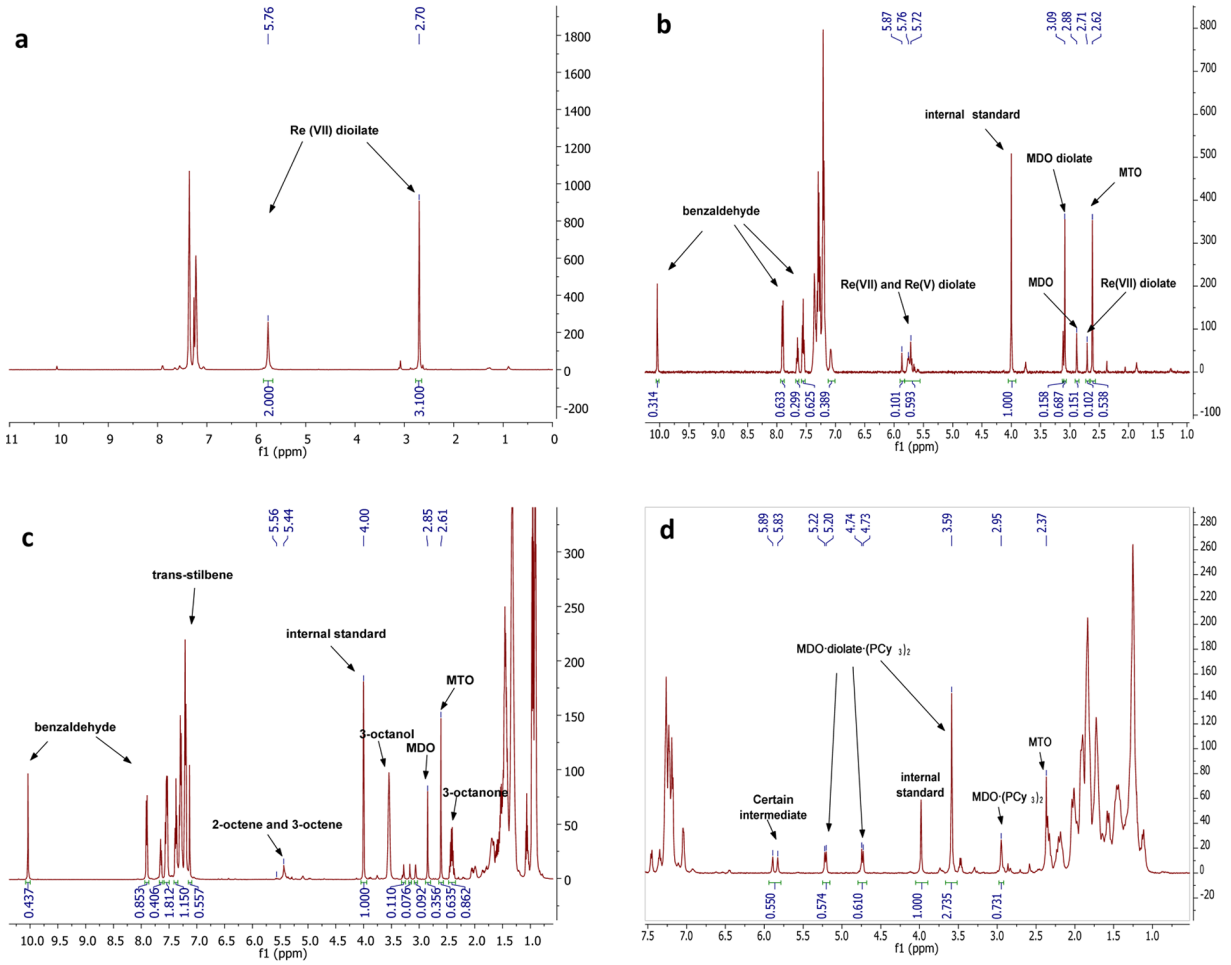

Figure 3. (a) ^{1}H NMR spectrum of Re(VII) diolate (**2**); (b) ^{1}H NMR spectrum of a solution of **2** after heating at 140 °C for 30 min; (c) ^{1}H NMR spectrum of the mixture in (b) with 3-octanol at 140 °C for 30 min; (d) ^{1}H NMR spectrum of the OAT reaction between Re(VII)·diolate (**2**) and MDO·$(PR_3)_2$ to give MDO·diolate·PR_3 and MTO. (The spectrum shown was acquired during the course of the reaction before completion. For more details, please refer to the Supporting Information.)

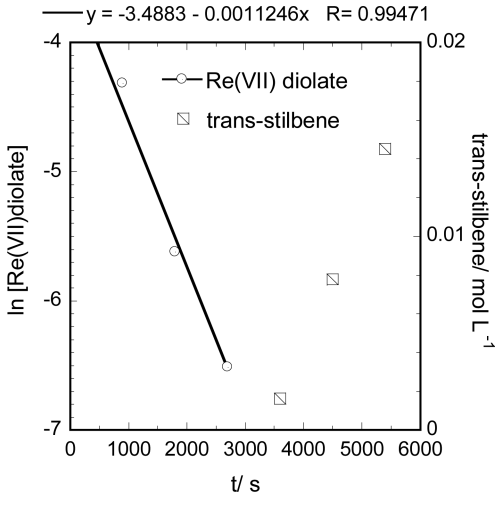

Figure 4. Kinetic profile for a heated solution of Re(VII)·diolate **2** at 140 °C over the course of ca. 2 h. The open circles represent the disappearance of Re(VII)·diolate **2**, which follows first-order dependence in [**2**] (solid line). The hatched squares represent *trans*-stilbene formation.

complexes emerges from the very unique and unusual rate dependence on total catalyst concentration $[Re]_T$ and is discussed in detail in a later section. The improved mechanism is shown in Scheme 3.

Rate-Determining Step. A series of NMR experiments were carried out at high catalyst loading (10 mol % MTO) to characterize catalytic species. The ^{1}H spectra at different times (2, 4, 6, 8, and 10 min) during the course of the reaction are displayed in Figure 5a. In addition to the methyl peak of MTO (CH_3ReO_3) at 2.5 ppm two other singlets are observed at 3.07 and 2.66 ppm, which are assigned to MDO·diolate (**4**), or one of its dinuclear forms $\mathbf{D}_2$ and $\mathbf{D}_3$, and Re^{VII}·diolate (**2**), respectively. Since the peak at 3.07 ppm is larger than the other two for the majority of the reaction, it is reasonable to assume that the reduction of MDO·diolate is the rate-determining step. Buildup in MTO as the reaction progresses is observed in open air and is attributed to oxidation of MDO and/or MDO·diolate under the reaction conditions (140 °C). For example, when the reaction is run with MDO·$(PCy_3)_2$ as the starting catalyst under inert atmosphere (N_2 or Ar), only 3.07 ppm (MDO·diolate or its dinuclear forms $\mathbf{D}_2$ and $\mathbf{D}_3$) is observed along with ca. 37% Re(VII)·diolate (**2**) (Figure 5b). Re(VII)·diolate is generated from slow disproportionation of MDO·diolate or its dinuclear compounds.

To discern the involvement of 3-octanol in the rate-determining step, we determined the kinetic isotope effect (KIE) using 3-D-octanol. The results are listed in Table 2. A

dx.doi.org/10.1021/om400127z | *Organometallics* XXXX, XXX, XXX–XXX

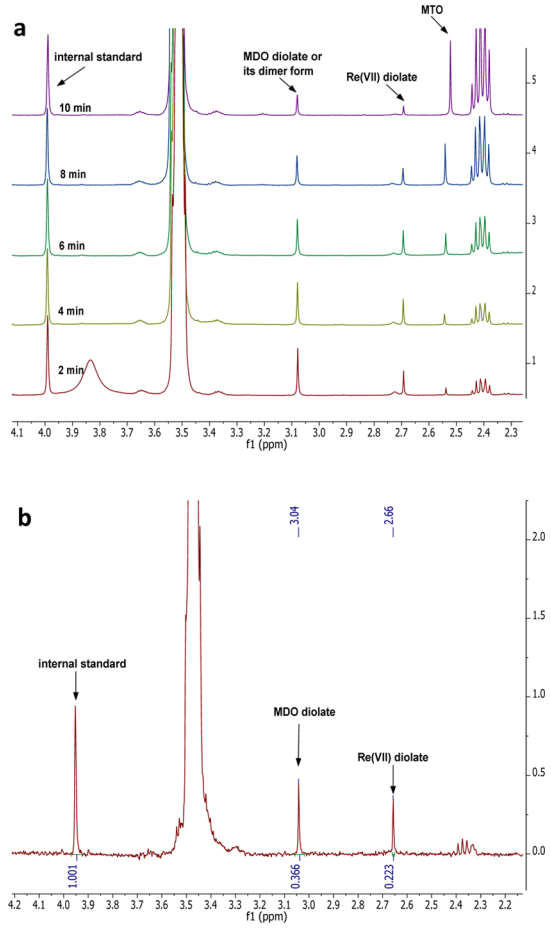

Figure 5. (a) ^{1}H NMR spectra acquired every 2 min using 10 mol % MTO in open air (preheating (*R*,*R*)-(+)-hydrobenzoin with 10 equiv 3-octanol to 140 °C, followed by addition of MTO (method A)); (b) ^{1}H NMR spectra of the reaction starting with MDO$(PCy_3)_2$ under Ar (1.25 mmol of (*R*,*R*)-(+)-hydrobenzoin with 12.5 mmol of 3-octanol and 10 mol % MDO$(PCy_3)_2$). Spectrum shown was acquired after 5 min.

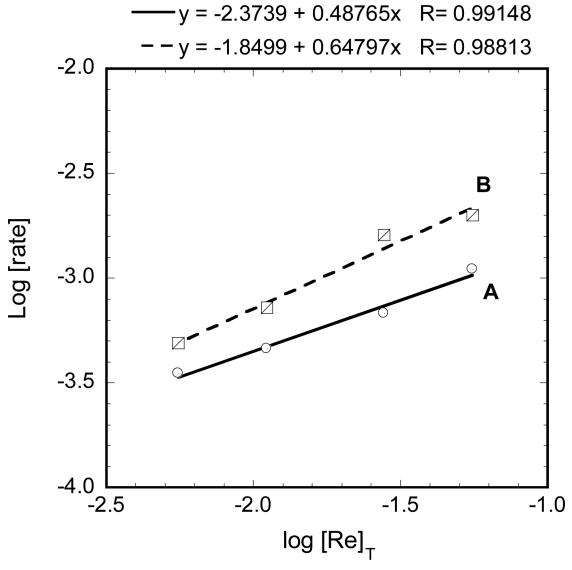

Figure 6. Reaction rate order dependence on $[Re]_T$, using methods A (open circles) and B (hatched squares).

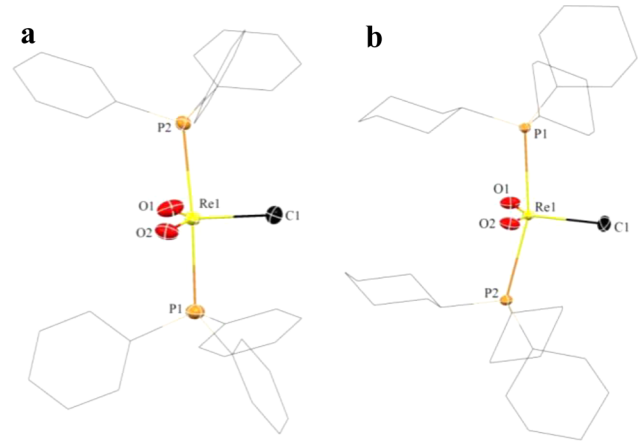

Figure 7. Thermal ellipsoid plots at the 50% level (H atoms have been omitted for clarity, in addition the PPH_3 and PCy_3 ligands have been depicted in wireframe) of (a) MDO·$(PPh_3)_2$. Selected bond lengths (Å) and angles (deg): Re1−O1, 1.745(2); Re1−O2, 1.780(3); Re1−C1, 2.114(5); Re1−P1, 2.4631(7); Re1−P2, 2.4691(6); P1−Re1−P2, 173.06(2); P1−Re1−O1, 86.35(7); P1−Re1−C1, 91.97(13); C1−Re1−O1, 114.68(18); O1−Re1−O2, 139.19(16). (b) MDO·$(PCy_3)_2$. Selected bond lengths (Å) and angles (deg): Re1−O1, 1.7493(10); Re1−O2, 1.7491(10); Re1−C1, 2.1294(15); Re1−P1, 2.4797(3); Re1−P2, 2.4881(3); P1−Re1−P2, 163.109(10); P1−Re1−O1, 88.69(3); P1−Re1−C1, 98.62(4); C1−Re1−O1, 108.02(7); O1−Re1−O2, 145.38(5).

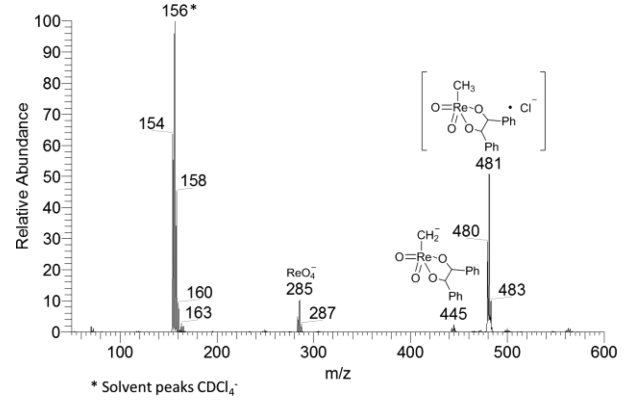

Figure 8. Mass spectrum of Re(VII) diolate **2** (formation of ReO_4^- is probably due to oxidation occurring under the APCI conditions).

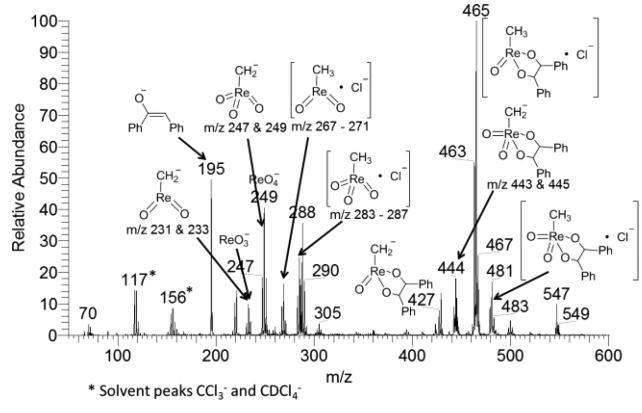

Figure 9. Mass spectrum of the mixture formed upon heating a Re(VII) diolate (**2**) solution at 140 °C for 30 min, showing the formation of MDO, MDO-diolate, and MTO.

dx.doi.org/10.1021/om400127z | *Organometallics* XXXX, XXX, XXX−XXX

Scheme 3. Improved Mechanism of the Major Pathways for MTO-Catalyzed DODH Reaction of Vicinal Diol in the Presence of Sacrificial Alcohol

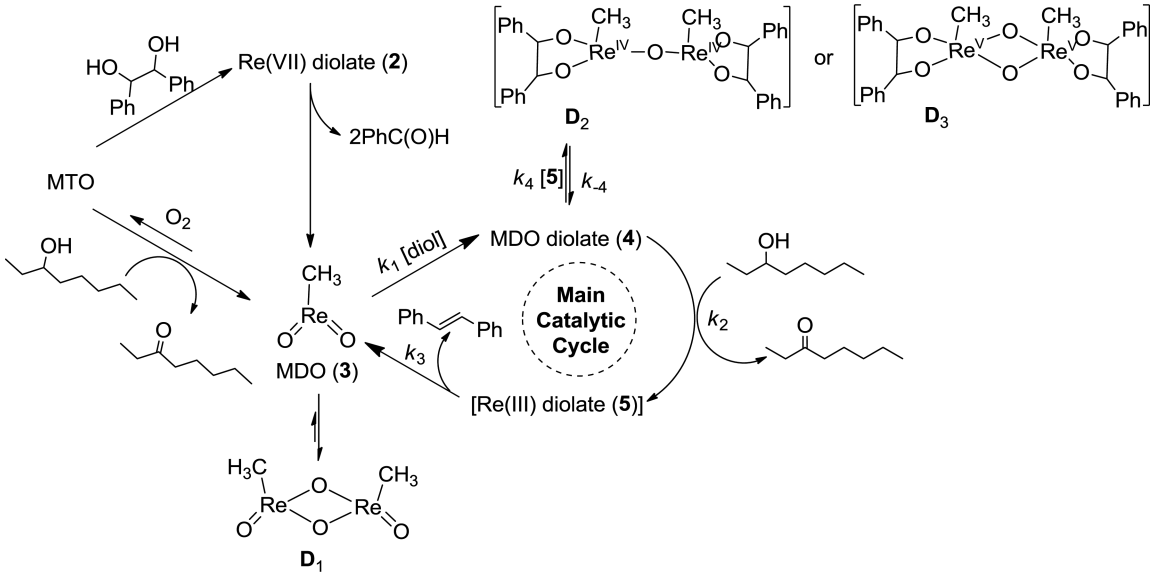

Table 2. Kinetic Isotope Reactions with Deuterated Alcohol, with 2 mol % MTO[a]

rate for 3-octanol (mol L^{-1} s^{-1})	rate for D-3-octanol (mol L^{-1} s^{-1})	KIE
4.56×10^{-4}	3.26×10^{-4}	1.4

[a]Both rates are measured as the slopes of reaction profiles according to method A, with MTO added last.

KIE of 1.4 is consistent with the reduction of MDO·diolate being rate-determining. The value of KIE being <2 can be rationalized in terms of alcohol coordination followed by H/D-transfer. A measure of KIE for the stoichiometric reaction of MDO(diolate)(PCy_3) also yielded a KIE of 1.2, consistent within experimental error with that observed for the catalytic reaction.

Thermodynamic activation parameters were determined from kinetic measurements at different temperatures, from 405 to 428 K (132−155 °C). The rate values obtained are as follows: 0.000 32 mol L^{-1} s^{-1} at 405 K, 0.000 46 mol L^{-1} s^{-1} at 413 K, 0.000 72 mol L^{-1} s^{-1} at 421 K, and 0.000 93 mol L^{-1} s^{-1} at 428 K. Activation parameters were obtained by least-squares fittings of the data to the Eyring equation, resulting in $\Delta H^{\ddagger}$ = 65 ± 14 kJ mol^{-1} and $\Delta S^{\ddagger}$ = −154 ± 33 J mol^{-1} K^{-1}. The large and negative entropy of activation is in good agreement with a bimolecular transition state.

Reaction Rate Order in Rhenium/Catalyst. Kinetic measurements of the reaction of hydrobenzoin in 3-octanol at different concentrations of MTO were carried out to determine the dependence on catalyst concentration. The results are listed in Table 3. Method A refers to addition of the MTO catalyst last, and method B to addition of hydrobenzoin last after incubation of MTO in 3-octanol at 140 °C for 10 min. The rate values were obtained from the slopes of the kinetic profiles as the reaction follows zeroth-order in [hydrobenzoin]. Plots of log of the rate versus log $[Re]_T$ revealed 0.49 and 0.65 order dependence in catalyst (Figure 6). This observation is in agreement with our hypothesis that MDO·diolate (**4**) forms a dinuclear complex with either Re(III) diolate to give $\mathbf{D}_2$ or itself to give $\mathbf{D}_3$ (Scheme 3). Either scenario is kinetically indistinguishable and manifests itself by giving a half-order dependence on $[Re]_T$. We illustrate herein the rate law derivation for involvement of $\mathbf{D}_2$ and using the rate constants given in Scheme 3 for the main catalytic cycle: $R_1 = -d[diol]/dt = k_1[MDO][diol]$; $R_2 = k_2[MDO\ diolate]$, alcohol is the solvent and thus $a_{alcohol} = 1$; $R_3 = k_3[Re(III)\ diolate]$.

Table 3. Rate Constants with Different [MTO] Using Methods A and B

[MTO] (mol %)	method A rate (mol L^{-1} s^{-1})	method B rate (mol L^{-1} s^{-1})
1	3.5×10^{-4}	4.9×10^{-4}
2	4.6×10^{-4}	7.2×10^{-4}
5	6.8×10^{-4}	1.6×10^{-3}
10	1.1×10^{-3}	2.0×10^{-3}

Assuming that all steps in the catalytic cycle contribute and $R_1 \approx R_2 \approx R_3$,

$$[Re(III)diolate] = \frac{k_2}{k_3}[MDO\ diolate]$$

$$[\mathbf{D}_2] = \frac{k_4}{k_{-4}}[MDO\ diolate][Re(III)\ diolate] = \frac{k_4 k_2}{k_{-4} k_3}[MDO\ diolate]^2$$

The mass balance is

$$[Re(III)\ diolate] + [MDO\ diolate] + [\mathbf{D}_2] + [MDO] = [Re]_T$$

$[MDO] \approx 0$, and if we assume that [Re(III) diolate] and [MDO diolate] are negligible compared to $[\mathbf{D}_2]$, then

$$[Re]_T \cong [D_2] = \frac{k_4 k_2}{k_{-4} k_3}[MDO\ diolate]^2$$

$$[MDO\ diolate] = \sqrt{\frac{k_{-4} k_3}{k_4 k_2}[Re]_T}$$

dx.doi.org/10.1021/om400127z | Organometallics XXXX, XXX, XXX−XXX

Hence, the approximate rate law is

$$-\frac{d[diol]}{dt} = R_2 = k_2[\text{MDO diolate}] = \sqrt{\frac{k_{-4}k_3}{k_4k_2}[\text{Re}]_T}$$

This derivation is consistent with the kinetic data as well as NMR observations that the majority of the catalyst is in a dimer form ($\mathbf{D}_1$, $\mathbf{D}_2$, or $\mathbf{D}_3$ in Scheme 3) and the rate constants k_2 and k_3 contribute to the catalytic rate of the reaction.

CONCLUSION

We have reported herein a thorough kinetics and mechanistic study on the deoxydehydration reaction of glycols using 3-octanol as a reductant and methyltrioxorhenium(VII) as catalyst. The reaction proceeds smoothly at 140−170 °C under ambient pressure and open to air to give *trans*-stilbene from (*R*,*R*)-(+)-hydrobenzoin and 3-octanone as the major products. The kinetics are zeroth-order in [hydrobenzoin] and half-order in [Re]. An induction period is observed when the catalyst is added last. However, if MTO and 3-octanol are allowed to react for 10 min at the reaction temperature, the induction period disappears. Two prevalent literature mechanisms were considered, probed, and refuted. Reactions of rhenium(VII) diolate revealed a novel C−C bond cleaving reaction that affords methyldioxorhenium(V) and benzaldehyde. Oxygen atom transfer from the rhenium(VII) diolate to MDO yields MTO and MDO·diolate. The latter did not produce the alkene product unless a reductant was added. All these findings and additional studies with MDO·$(PR_3)_2$ support a catalytic cycle in which MDO·diolate is reduced by 3-octanol to a transient rhenium(III) diolate, which is responsible for alkene extrusion and regeneration of MDO (Schemes 2 and 3). The $[Re]^{1/2}$ dependence is rationalized by formation of a dinuclear rhenium complex ($\mathbf{D}_2$) (Scheme 3). Our investigation offers a new mechanism for DODH using oxorhenium catalysis that is quite different from the prevalent rhenium(VII) and rhenium(V) cycles that have been claimed in the literature (Scheme 1). Our new mechanism should stimulate future catalyst design on the basis of a rhenium(V)/rhenium(III) cycle.

EXPERIMENTAL METHODS

General Information. All commercial materials were used as received without further purification unless specified. (*R*,*R*)-(+)-Hydrobenzoin, 3-octanol, (*S*,*S*)-hydrobenzoin, *meso*-hydrobenzoin, *cis*-stilbene oxide, styrene oxide, 1-phenyl-1,2-ethanediol, erythritol, 2-nonanol, 5-nonanol, 1-heptanol, cyclohexanol, *cis*-1,2-cyclooctanediol, *trans*-1,2-cyclooctanediol, and 1,2-decanediol were purchased from Sigma-Aldrich. Methyltrioxorhenium, ReO_3, Re_2O_7, and NH_4ReO_4 were purchased from Strem Chemicals. MTO was purified by vacuum sublimation at 40 °C. ^{1}H NMR and ^{13}C NMR were recorded with a Bruker Avance ARX-400. HMQC and ^{2}H NMR were recorded with Bruker Avance DRX-500 spectrometers. The GC analysis was performed using an Agilent Technologies 6890 N with a DB-5 column.

Generation of $MeRe^{VII}O_2(OCHPhCHPhO)$ (2). (*R*,*R*)-(+)-Hydrobenzoin (25.7 mg, 0.12 mmol) was added to a solution of methyltrioxorhenium (27.4 mg, 0.11 mmol) in 2 mL of dry methylene chloride in the presence of molecular sieves. After 24 h at room temperature (under a nitrogen atmosphere), the solution inside the NMR tube changed from colorless to yellow to deep red. NMR analyses showed formation of Re(VII) diolate (**2**). ^{1}H NMR (400 MHz, $CDCl_3$): δ 7.10−7.40 ppm (m), 5.75 (br s, 2 H), 2.70 (s, 3 H). ^{13}C NMR (500 MHz, $CDCl_3$): δ 128.97, 128.80, 126.54, 108.82, 40 ppm (coupled to CH_3).

General Procedure for Kinetics. The glycol (2.5 mmol, referred to (*R*,*R*)-(+)-hydrobenzoin in most cases) was mixed with the sacrificial alcohol (25 mmol, referred to 3-octanol most of the time) and diphenylmethane (∼0.25 mmol, internal standard) in a three-neck round-bottom flask. After refluxing the reaction mixture at 140 °C in a preheated silicone oil bath, CH_3ReO_3 (0.05 mmol, 2 mol %) was added, which marked the starting point of the kinetic data collection. Aliquots were taken at different time points, quenched immediately in $CDCl_3$ over ice, and analyzed by ^{1}H NMR spectroscopy (or GC) to generate kinetic profiles of concentration versus time.

Synthesis of $MeRe^{V}O_2(PPh_3)_2$. A solution of MTO (100 mg, 0.40 mmol) in 2 mL of dry diethyl ether was treated with a solution of PPh_3 (631 mg, 2.4 mmol) in 3 mL of dry diethyl ether under a nitrogen atmosphere. Over 24 h at room temperature, the solution changed from colorless to deep orange, and the orange product crystallized out of the diethyl ether solution. The solid was filtered and washed with dry diethyl ether three times to yield pure MDO·$(PPh_3)_2$ (175.7 mg, 58% yield). Anal. Calcd for $C_{37}H_{33}O_2P_2Re$: C, 58.64; H, 4.39. Found: C, 57.66; H, 4.39. The complex is not solution stable. Therefore, generation of the complex *in situ* allowed for spectroscopic characterization (see below).

Preparation of $MeRe^{V}O_2(PPh_3)_2$ *in Situ*. A solution of MTO (31 mg, 0.125 mmol) in 1 mL of $CDCl_3$ was treated with PPh_3 (98 mg, 0.375 mmol). After 1 h 30 min at ∼35 °C or 38 h at room temperature (under a nitrogen atmosphere), the solution changed from colorless to yellow to deep red. ^{31}P NMR analyses showed formation of $OPPh_3$. ^{31}P NMR (400 MHz,$CDCl_3$): δ 30 ($OPPh_3$, 32%), 10 (coordinated PPh_3, 41%), −5 (PPh_3, 27%). ^{1}H NMR (400 MHz, $CDCl_3$): δ 2.85 (s, 3 H). ^{13}C NMR (400 MHz, $CDCl_3$): δ 143 ppm.

Synthesis of $MeRe^{V}O_2(PCy_3)_2$. A solution of MTO (100 mg, ∼0.4 mmol) in 2 mL of dry diethyl ether was treated with a solution of PCy_3 (675 mg, 2.4 mmol) in 3 mL of dry diethyl ether under a nitrogen atmosphere. Over 24 h at room temperature, the solution changed from colorless to deep orange, and the orange product precipitated out of the diethyl ether solution. The solid was filtered and washed with dry diethyl ether three times to yield pure $MeRe^{V}O_2(PCy_3)_2$ (140.3 mg, 44% yield). ^{31}P NMR (400 MHz, $CDCl_3$): δ 8 (coordinated PCy_3). ^{1}H NMR (400 MHz, $CDCl_3$): δ 3.0 (s, 3 H) ppm, 1.1−2.3 ppm (cyclohexyl peaks). ^{13}C NMR (400 MHz, $CDCl_3$): δ 140 ppm (coupled to CH_3), 34, 29, 27, 26 ppm (cyclohexyl peaks). Anal. Calcd for $C_{37}H_{69}O_2P_2Re$: C, 55.96; H, 8.76. Found: C, 55.69; H, 8.80.

X-ray Structures of $MeRe(O)_2(PPh_3)_2$ and $MeRe(O)_2(PCy_3)_2$. Details and general procedure for X-ray determination are provided in the Supporting Information. ORTEP diagrams of both structures with selected bond lengths and angles are presented in Figure 7.

Mass Spectrometry. All mass spectrometric experiments were carried out in a Thermo Scientific linear quadrupole ion trap (LQIT)−Fourier transform ion cyclotron resonance (FT-ICR; 7 T magnet) mass spectrometer. The nominal pressures of the LQIT vacuum manifold and the FT-ICR vacuum manifold were maintained at about 0.60×10^{-5} Torr and 2.0×10^{-10} Torr, respectively, as read by ion gauges. The LQIT-FT-ICR mass spectrometer was operated using the LTQ Tune Plus interface.

An atmospheric pressure chemical ionization (APCI) source was used for ion generation. Reaction mixtures in $CDCl_3$ were diluted 100-fold with dry $CDCl_3$ in a glovebox. $CDCl_3$ was used, as it was the solvent for NMR measurements, and it encouraged negative ion production. The diluted solutions were directly introduced into the APCI source by using a Hamilton gastight syringe operating at a flow rate of 20 μL/min. APCI discharge current was 4.0 μA. The vaporizer temperature was set at 80 or 120 °C for optimized ion signals. Sheath and auxiliary gas (N_2) flows were 35 and 5 (arbitrary units), respectively. A heated ion transfer capillary/mass spectrometer inlet temperature of 275 °C was used. All dc voltages and offsets for the ion optics were optimized utilizing the integrated tuning features of the LTQ Tune Plus interface. Xcalibur 2.0 software was used for data analysis. All LQIT mass spectra acquired were an average of 40 scans. Figure 8 shows MS characterization of MTO-diolate (**2**), and Figure 9 the reaction mixture resulting from heating complex **2** at 140 °C.

dx.doi.org/10.1021/om400127z | *Organometallics* XXXX, XXX, XXX−XXX

■ ASSOCIATED CONTENT

Supporting Information

Kinetics details and NMR spectra for the DODH reactions; UV−vis and TEM images of Re NPs formed in 3-octanol; synthesis and full characterizations of $MDO(PR_3)_2$ complexes; X-ray characterizations of $MDO(PR_3)_2$ (R = Ph and Cy) (CIF); preparation and full characterization by NMR including HMQC of MTO(diolate) and $MDO(diolate)(PCy_3)_2$; details and spectral characterization on the inert-metal OAT between MTO(diolate) and MDO; and results on DODH in the absence of a sacrificial alcohol. This material is available free of charge via the Internet at http://pubs.acs.org.

■ AUTHOR INFORMATION

Corresponding Author

*E-mail: mabuomar@purdue.edu.

Present Address

[§]Department of Chemistry, College of Science, Gaziosmanpasa University, Tasliciftlik, 60240, Tokat, Turkey.

Author Contributions

All authors have given approval to the final version of the manuscript.

Funding

Notes

The authors declare no competing financial interest.

■ ACKNOWLEDGMENTS

S.L. and M.M.A.-O. wish to thank Dr. Grigori Medvedev and Ms. Silei Xiong of Purdue University for useful discussions on kinetics. A.S. acknowledges support from TUBITAK International Postdoctoral Research Scholarship Programme. E.A.I. acknowledges the National Science Foundation via the CAREER Award (CHE-0955636) for funding. L.Y. and the described MS studies were supported as part of the Center for Direct Catalytic Conversion of Biomass to Biofuels (C3Bio), an Energy Frontier Research Center (EFRC) funded by the U.S. Department of Energy, Office of Science, Office of Basic Energy Sciences, under award number DE-SC-0000997. This research was supported by the U.S. Department of Energy, Basic Energy Sciences (DOE-BES grant number DE-FG-02-06ER15794).

■ REFERENCES

(1) (a) Huber, G. W.; Iborra, S.; Corma, A. *Chem. Rev.* **2006**, *106*, 4044. (b) Serrano-Ruiz, J. C.; Luque, R.; Sepulveda-Escribano, A. *Chem. Soc. Rev.* **2011**, *40*, 5266. (c) Alonso, D. M.; Bond, J. Q.; Dumesic, J. A. *Green Chem.* **2010**, *12*, 1493. (d) Gallezot, P. *Chem. Soc. Rev.* **2012**, *41*, 1538. (e) Huber, G. W.; Corma, A. *Angew. Chem., Int. Ed.* **2007**, *46*, 7184. (f) Chheda, J. N.; Huber, G. W.; Dumesic, J. A. *Angew. Chem., Int. Ed.* **2007**, *46*, 7164.

(2) (a) Herrmann, W. A.; Kühn, F. E. *Acc. Chem. Res.* **1997**, *30*, 169. (b) Rudolph, J.; Reddy, K. L.; Chiang, J. P.; Sharpless, K. B. *J. Am. Chem. Soc.* **1997**, *119*, 6189. (c) Jonsson, S. Y.; Färnegårdh, K.; Bäckvall, J.-E. *J. Am. Chem. Soc.* **2001**, *123*, 1365.

(3) (a) Gable, K. P. *Organometallics* **1994**, *13*, 2486. (b) Zhu, Z.; Espenson, J. H. *J. Mol. Catal. A: Chem.* **1995**, *103*, 87. (c) Gable, K. P.; Brown, E. C. *Organometallics* **2000**, *19*, 944.

(4) Cook, G. K.; Andrews, M. A. *J. Am. Chem. Soc.* **1996**, *118*, 9448.

(5) Ziegler, J. Z.; Zdilla, M. J.; Evans, A. J.; Abu-Omar, M. M. *Inorg. Chem.* **2009**, *48*, 9998.

(6) Arceo, E.; Ellman, J. A.; Bergman, R. G. *J. Am. Chem. Soc.* **2010**, *132*, 11408.

(7) (a) Ahmad, I.; Chapman, G.; Nicholas, K. M. *Organometallics* **2011**, *30*, 2810. (b) Vkuturi, S.; Chapman, G.; Ahmad, I.; Nicholas, K. M. *Inorg. Chem.* **2010**, *49*, 4744.

(8) Sousa, S. C. A.; Fernandes, A. C. *Tetrahedron Lett.* **2011**, *52*, 6960.

(9) Yi, J.; Liu, S.; Abu-Omar, M. M. *ChemSusChem* **2012**, *5*, 1401.

(10) Shiramizu, M.; Toste, F. D. *Angew. Chem., Int. Ed.* **2012**, *51*, 8082.

(11) (a) Thibault, M. E.; DiMondo, D. V.; Jennings, M.; Abdelnur, P. V.; Eberlin, M. N.; Schlaf, M. *Green Chem.* **2011**, *13*, 357. (b) Schlaf, M.; Ghosh, P.; Fagan, P. J.; Hauptman, E.; Bullock, R. M. *Adv. Synth. Catal.* **2009**, *351*, 789. (c) Ghosh, P.; Fagan, P. J.; Marshall, W. J.; Hauptman, E.; Bullock, R. M. *Inorg. Chem.* **2009**, *48*, 6490.

(12) Stanowski, S.; Nicholas, K. M.; Srivastava, R. S. *Organometallics* **2012**, *31*, 515.

(13) (a) Zhu, Z. L.; Espenson, J. H. *J. Org. Chem.* **1996**, *61*, 324. (b) Herrmann, W. A.; Roesky, P. W.; Wang, M.; Scherer, W. *Organometallics* **1994**, *13*, 4531. (c) Gable, K. P.; Phan, T. N. *J. Am. Chem. Soc.* **1994**, *116*, 833. (d) Gable, K. P.; Juliette, J. J. J. *J. Am. Chem. Soc.* **1995**, *117*, 955. (e) Gable, K. P.; AbuBaker, A.; Zientara, K.; Wainwright, A. M. *Organometallics* **1999**, *18*, 173.

(14) Korstanje, T. J.; Jastrzebski, J. T. B. H.; Gebbink, R. J. M. K. *ChemSusChem* **2010**, *3*, 695.

(15) (a) Biswas, K.; Rao, C. N. R. *J. Phys. Chem. B* **2005**, *110*, 842. (b) Ghosh, S.; Biswas, K.; Rao, C. N. R. *J. Mater. Chem.* **2007**, *17*, 2412.

(16) (a) Gomez, M.; Favier, I. "Metal Nanoparticles Dispersed in Solution: Tests to Identify the Catalyst Nature. In *Metal Nanoclusters in Catalysis and Materials Science: The Issue of Size Control*; Corain, B.; Schmid, G.; Toshima, N., Eds.; Elsevier, 2008; p 427. (b) Borowski, A. F.; Sabo-Etienne, S.; Chaudret, B. *J. Mol. Catal. A: Chem.* **2001**, *174*, 69. (c) Georgiades, G. C.; Sermon, P. A. *J. Chem. Soc., Chem. Commun.* **1985**, 975.

(17) (a) Zhu, Z. L.; AlAjlouni, A. M.; Espenson, J. H. *Inorg. Chem.* **1996**, *35*, 1408. (b) Haider, J. J.; Kratzer, R. M.; Herrmann, W. A.; Zhao, J.; Kühn, F. E. *J. Organomet. Chem.* **2004**, *689*, 3735.

(18) (a) Zhang, X.; Chen, X.; Chen, P. *Organometallics* **2004**, *23*, 3437. (b) Jackson, S. M.; Chisholm, D. M.; McIndoe, J. S.; Rosenberg, L. *Eur. J. Inorg. Chem.* **2011**, *2011*, 327.

(19) (a) Conry, R. R.; Mayer, J. M. *Inorg. Chem.* **1990**, *29*, 4862. (b) McPherson, L. D.; Drees, M.; Khan, S. I.; Strassner, T.; Abu-Omar, M. M. *Inorg. Chem.* **2004**, *43*, 4036. (c) Ison, E. A.; Cessarich, J. E.; Travia, N. E.; Fanwick, P. E.; Abu-Omar, M. M. *J. Am. Chem. Soc.* **2007**, *129*, 1167.

(20) (a) Smeltz, J. L.; Boyle, P. D.; Ison, E. A. *J. Am. Chem. Soc.* **2011**, *133*, 13288. (b) Lilly, C. P.; Boyle, P. D.; Ison, E. A. *Organometallics* **2012**, *31*, 4295.

(21) Qu, S.; Dang, Y.; Wen, M.; Wang, Z.-X. *Chem.—Eur. J.* **2013**, *19*, 3827.

(22) (a) Abu-Omar, M. M.; Appelman, E. H.; Espenson, J. H. *Inorg. Chem.* **1996**, *35*, 7751. (b) Herrmann, W. A.; Fischer, R. W.; Scherer, W. *Adv. Mater.* **1992**, *4*, 653. (c) Hermann, W. A.; Fischer, R. W. *J. Am. Chem. Soc.* **1995**, *117*, 3223. (d) Espenson, J. H.; Yiu, D. T. Y. *Inorg. Chem.* **2000**, *39*, 4113.